

**Radomir Jovičić**

University of Belgrade  
Faculty of Mechanical Engineering  
Innovation Center

**Aleksandar Sedmak**

Full Professor  
University of Belgrade  
Faculty of Mechanical Engineering

**Zijah Buržić**

Military Institute, Zarkovo

**Vencislav Grabulov**

Military Institute, Zarkovo

**Jasmina Lozanović**

University of Belgrade  
Faculty of Mechanical Engineering  
Innovation Center

# Structural Integrity Assessment of Ferritic-Austenitic Welded Joints

In this paper the influence of cracks on structural integrity of heterogeneous ferrite-austenite welded joints applying the basic fracture mechanics concept was analysed. The crack driving force was obtained numerically using King's method, while materials resistance to crack growth was determined experimentally via J-integral and was given as the J-R curve. In order to find out properties of such welded joints, plates made of high alloyed austenite steel were welded to plates made of microalloyed ferrite steel. The experimental investigation, in combination with the numerically obtained results, enabled reliable estimation of structural integrity of ferrite-austenite welded joints.

**Keywords:** ferrite-austenite welded joints, fracture mechanics, structural integrity, cracking phenomena, weldment heterogeneity.

## 1. INTRODUCTION

High strength low alloyed (HSLA) ferrite steels are increasingly used for welded constructions due to their high strength and toughness, as well as good weldability. Their typical application is for low temperature pressure vessels, as in the case of CO<sub>2</sub> storage tanks, made by welding of rolled and bended plates. At the same time, since attachments like small pipes are not produced of these steels, another type of steel has to be used, like high alloyed ausenite steels, also suitable for the low temperature applications. Anyhow, such a combination of steels causes another problem, related to the welding of different types of steels. Namely, both ferrite and austenite steels are prone to different types of cracking, like cold, lamellar, hot cracking, and especially due to their different physical and mechanical properties their heterogeneous welded joints are even more susceptible to all types of cracking.

Therefore, in this paper the influence of cracks on structural integrity of heterogeneous welded joints applying the concept of fitness-for-purpose was analysed, as described by Jovicic in [1,2]. To this end, the fracture mechanics basic concept has been applied, namely the crack driving force has been compared with the material resistance to the crack growth. The crack driving force has been obtained numerically using King's method [3], while materials resistance to crack growth has been determined experimentally via J-integral and given as the J-R curve.

## 2. CRACKING PHENOMENA IN FERRITE-AUSTENITE JOINTS

Typical problems with welded joints made of HSLA ferrite steels are toughness reduction, nil ductility temperature increase, cold cracking and brittle fracture

Received: March 2008, Accepted: May 2008

Correspondence to: Dr Aleksandar Sedmak  
Faculty of Mechanical Engineering,  
Kraljice Marije 16, 11120 Belgrade 35, Serbia  
E-mail: asedmak@mas.bg.ac.yu

can occur. On the other hand, typical problem with welded joints made of high alloyed austenite steels are coarse grain structure, σ-phase, hot cracking, intercrystal corrosion and strength reduction. Furthermore, if heterogeneous joints are to be made of these two types of steels, it has to be take into account that austenite steel has 100 °C lower melting temperature, 20 % higher specific heat, 3 times lower heat conductivity, 5 times higher electrical resistance, 50 % higher thermal linear coefficient, and significantly higher solubility of hydrogen.

In order to avoid the mentioned problems, the Scheffler's diagram can be used. Basically, this diagram enables the right choice of the filler metal in order to avoid all problems typical for ferrite-austenite welded joints: cold cracking (martensite), hot cracking (austenite), embrittlement (δ-ferrite) and its combination (A+M), Fig. 1. Practical application is illustrated by points A-D, as follows: point A corresponds to the ferrite base metal – HSLA steel NIOVAL 47-ČRN 460 (JUS), point B to the austenite base metal – X7CrNiNb18.10 (DIN), so that point C presents the average content of their 50 – 50 % mixture, being the input value for filler metal choice. Filler metal – INOX R 29/9, steelworks Jesenice, was chosen (point D) in such a way that the point E, corresponding to the weld metal (WM) composition, falls into the "white" region, being outside of all critical regions in diagram, as shown in Figure 1.

### 2.1 Storage tank for CO<sub>2</sub> – cracking phenomena

The storage tank for CO<sub>2</sub> has been tested recently, during regular inspection period, as described in more details in [2]. The storage tank is cylindrical, horizontal, diameter 1600 mm, total length 7180 mm and volume 12.5 m<sup>3</sup>, Fig. 2. Its body has been made of HSLA ferrite steel NIOVAL 47-ČRN 460 (JUS) of thickness 14 mm, while the attachments and revision opening flange have been made of high alloyed austenite steel X7CrNiNb18.10 (DIN). The lowest operating temperature is – 55 °C, the highest pressure 30 bars, testing pressure 39 bars.

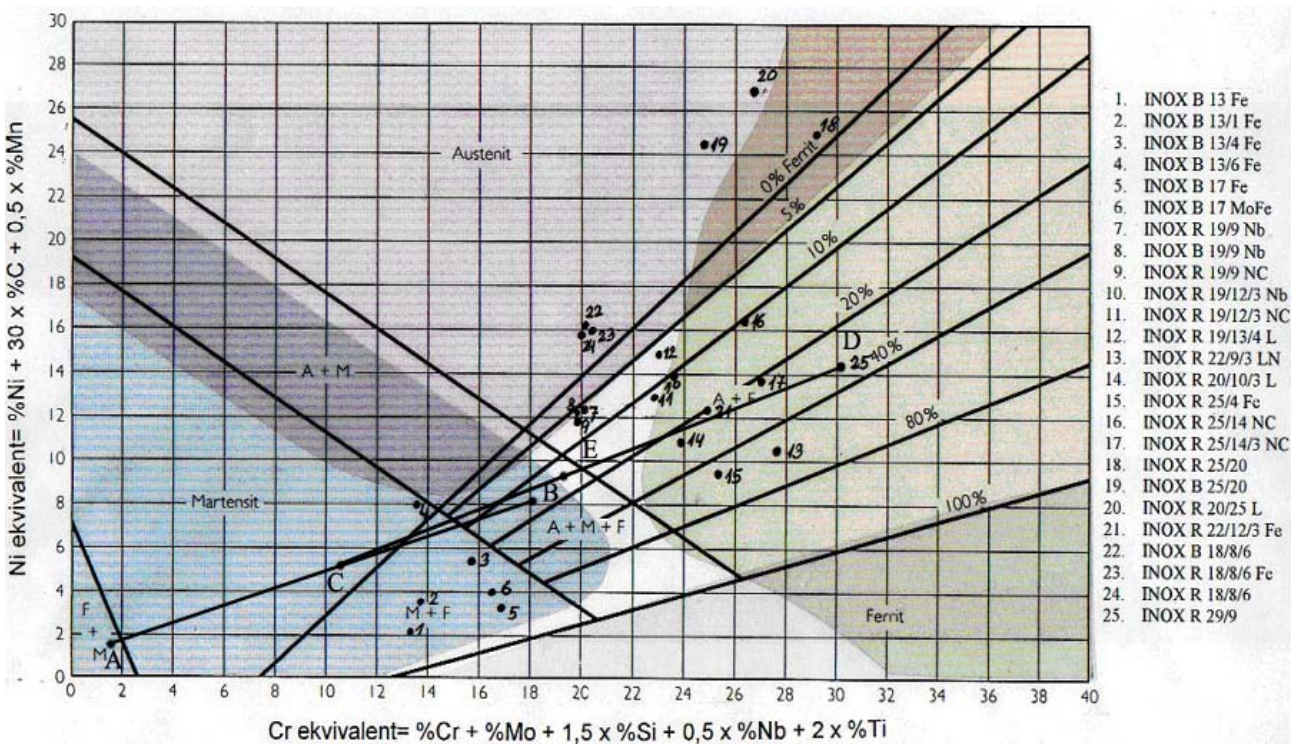


Figure 1. Scheffler diagram

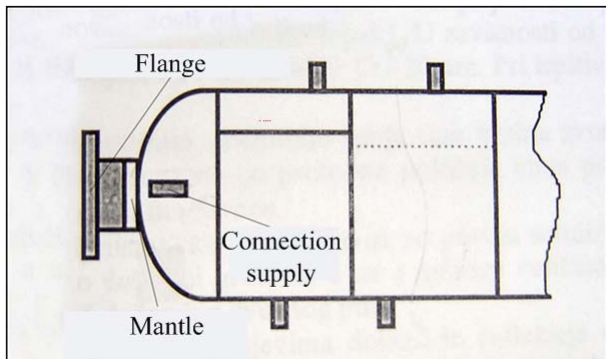


Figure 2. The storage tank for  $\text{CO}_2$

Different non-destructive-testing (NDT) methods have been applied, revealing pores at the inner side of flange, Fig. 3, and cracks at the outer side of flange, Fig. 4. Replicas revealed microcracks in heat-affected-zone (HAZ) of microalloyed steel, length 1.8 mm, Fig. 5, and cold cracks (longitudinal: length 60, 46 & 9 mm, depth cca 3.5 mm; radial: length 10, 9 & 5 mm, depth cca 6.5 mm), Fig. 6. The coarse grain structure and traces of martensite in beinite structure have been identified as well. Microstructure of WM is austenite with cca 35 %  $\delta$ -ferrite. The hydro test revealed two through-the-thickness cracks at the outer side of flange.

### 3. SIMPLIFIED KING'S SPRING LINE MODEL

Basic assumptions of King's spring line model are:

- surface crack is positioned in flat infinite plate loaded by remote tension,
- real crack front is replaced with quadrangle, with constant depth,  $c = \text{const.}$ ,
- spring is elastic-ideal plastic,
- Dagdale model is applied to take into account plasticity at the crack tip.



Figure 3. Pores at the inner side of flange



Figure 4. Cracks in a flange welded joint

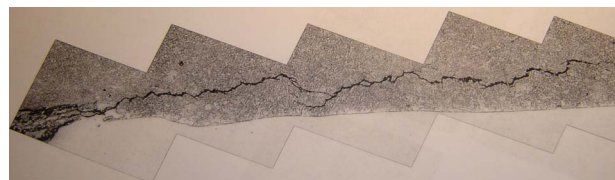


Figure 5. Microcracks in HAZ of microalloyed steel

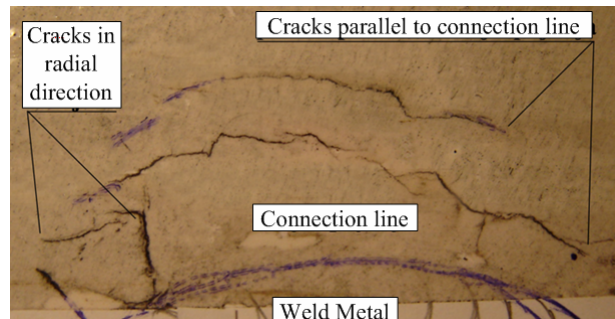


Figure 6. Cold cracking

Thus, denoting by  $\sigma_c = N/h$  membrane loading and by  $m = M/(h^2/6)$  bending loading, one can get:

$$\delta = \frac{4a}{E}(\sigma - \sigma_c), \quad (1)$$

$$\theta = \frac{-8(1+\nu)a}{(3+\nu)Eh}m. \quad (2)$$

On the other hand side it is obvious that:

$$\delta = \frac{2(1-\nu^2)h}{E}(C_{11}\sigma_c + C_{12}m), \quad (3)$$

$$\theta = \frac{12(1-\nu^2)h}{E}(C_{12}\sigma_c + C_{22}m). \quad (4)$$

By eliminating  $\delta$  and  $\theta$  from (1) – (4), it follows:

$$\sigma_c = \frac{2}{1-\nu^2} \frac{a}{hD} \left[ C_{22} + \frac{2}{3(1+\nu)(3+\nu)} \frac{a}{h} \right] \sigma = \alpha\sigma, \quad (5)$$

$$m = -\frac{2}{1-\nu^2} \frac{a}{hD} C_{12}\sigma = -\beta\sigma, \quad (6)$$

with

$$D = \left( C_{11} + \frac{2}{1-\nu^2} \frac{a}{h} \right) \left[ C_{22} + \frac{2}{3(1+\nu)(3+\nu)} \frac{a}{h} \right] - C_{12}^2. \quad (7)$$

Spring remains elastic until yielding point. As the yielding criterion a simple expression is used:

$$\sigma_c = \frac{h-c}{h}\sigma_F. \quad (8)$$

Thus, the yielding appears when the average stress in the ligament reaches stress,  $\sigma_F$ , defined as:

$$\sigma_F = \frac{\sigma_y + \sigma_m}{2}. \quad (9)$$

From (7), the expression for the ligament yield stress,  $\sigma_{LY}$ , follows:

$$\sigma_{LY} = \frac{1}{\alpha} \left( 1 - \frac{c}{h} \right) \sigma_F. \quad (10)$$

After yielding plasticity at the crack tips is taken into account by using the “effective” crack length,  $a_p = a + r_y$ , where  $r_y$  stands for the plastic zone size. Based on that and by applying Dugdale ligament yield model, Fig. 7, one gets:

$$\sin \frac{\pi a_p}{w} = \frac{\sin \frac{\pi a}{w}}{\cos \frac{\pi}{2} \frac{\sigma - \sigma_c}{\sigma_F - \sigma_c}} = \frac{\sin \frac{\pi a}{w}}{\cos \frac{\pi}{2} \left[ \frac{h}{c} \frac{\sigma}{\sigma_F} - \left( \frac{h}{c} - 1 \right) \right]}, \quad (11)$$

where  $w$  stands for the plate width. The plate can sustain loading until yielding reaches its ends, defined by net yield stress,  $\sigma_{NSY}$ , as follows from (9) with  $a_p = w/2$ :

$$\sigma_{NSY} = \sigma_F \left( 1 - \frac{2a}{w} \frac{c}{h} \right). \quad (12)$$

One should notice that King’s model is valid for a finite width plate. Anyhow, if  $w \rightarrow \infty$ ,  $\sin(\sigma a_p/w) \approx \sigma a_p/w$  and  $\sin(\sigma a/w) \rightarrow \sigma a/w$  one gets the approximate solution for an infinite plate:

$$a_p = \frac{a}{\cos \frac{\pi}{2} \left[ \frac{h}{2} \frac{\sigma}{\sigma_F} - \left( \frac{h}{c} - 1 \right) \right]} \text{ and } \sigma_{NSY} \cong \sigma_F, \quad (13)$$

which can be applied for the thin shell with small curvature, like the large sphere.

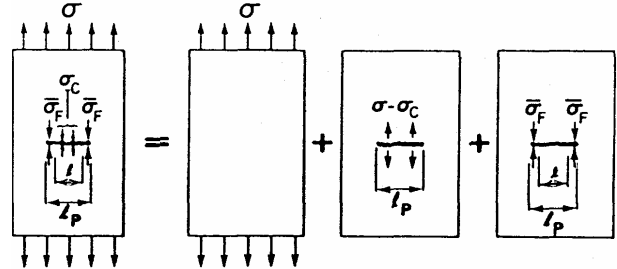


Figure 7. Ligament yield model

Since  $\sigma_c$  and  $m$  are now defined for the whole range of the remote stress  $\sigma$ , COD and J can be evaluated as follows (see also Figure 8):

$$CTOD = \delta + \theta(h - 2C), \quad (14)$$

$$CMOD = \delta + \theta h. \quad (15)$$

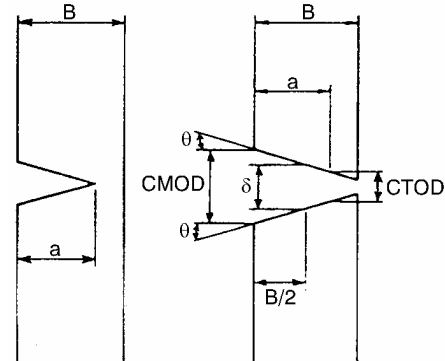


Figure 8. Calculation of CMOD and CTOD

By substituting expressions for  $\delta$ ,  $\theta$  one gets ( $\sigma \leq \sigma_{LY}$ ):

$$CTOD = \frac{4a\sigma}{E} \left[ 1 + \left( \frac{2(1+\nu)}{3+\nu} \frac{h-2C}{h} \beta - \alpha \right) \right], \quad (16)$$

$$CMOD = \frac{4a\sigma}{E} \left[ 1 + \left( \frac{2(1+\nu)}{3+\nu} \beta - \alpha \right) \right], \quad (17)$$

i.e. ( $\sigma_{LY} < \sigma < \sigma_{NSY}$ ),

$$CTOD = \frac{4(a+r_y)}{E} (\sigma - \sigma_{LY}) + CTOD_{LY} \left( \frac{a+r_y}{a} \right), \quad (18)$$

$$CMOD = \frac{4(a+r_y)}{E} (\sigma - \sigma_{LY}) + CMOD_{LY} \left( \frac{a+r_y}{a} \right). \quad (19)$$

To calculate J, for  $\sigma < \sigma_{LY}$  one can use the linear elastic fracture mechanics relation:

$$J_c = \frac{1-\nu^2}{E} K_I^2 = \frac{1-\nu^2}{E} h (\sigma_c F_1 + m F_2)^2, \quad (20)$$

where  $F_1$  and  $F_2$  are defined in [3]. For  $\sigma_{LY} < \sigma < \sigma_{NSY}$ ,  $J_p$  can be calculated by using load line displacement:

$$J_p = - \int_{\delta_{LY}}^{\delta} \frac{\partial N}{\partial c} d\delta - \int_{\delta_{LY}}^{\delta} \frac{\partial M}{\partial c} d\theta, \quad (21)$$

where for  $\partial N/\partial c = -\sigma_F$ ,  $\partial M/\partial c = 0 \Rightarrow$

$$J_p = \sigma_F (\delta - \delta_{LY}) = \frac{4\sigma_F}{E} \left[ (a + r_y) \sigma - a \sigma_{LY} - \frac{h-c}{h} r_y \sigma_F \right]. \quad (22)$$

#### 4. FRACTURE MECHANICS AND STRUCTURAL INTEGRITY OF WELDMENTS

Basic fracture mechanics parameters, applicable to weldments, are the crack tip opening displacement (CTOD) and J integral [3]. By using these parameters, the structural integrity of weldments, as described in [3], can be assessed by comparing the crack driving forces (CDF), vs J-R curve. The most suitable (simple) method for CDF evaluation in the case analysed in this paper is the line spring King's method, which is based on CTOD analysis of large flat plates with a surface crack [3], whereas J-R curves can be obtained in standard experimental way [4]. By applying King's model, one can get the set of CDFs, as described in [3].

Standard fracture mechanics testing includes J-R curve evaluation by using partial unloading technique and applying it to the welded joint, as described in ASTM E1820 [4], including specimen geometry, Fig. 9.

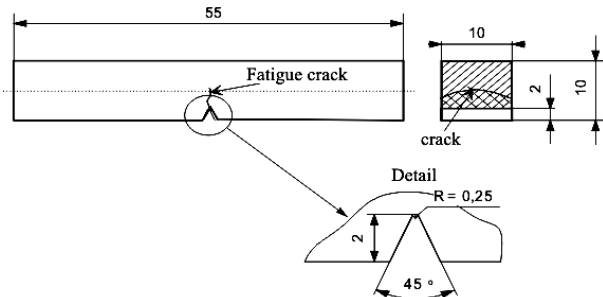


Figure 9. Specimen for J-R curve testing

#### 5. RESULTS OF FRACTURE MECHANICS TESTING AND STRUCTURAL INTEGRITY ASSESSMENT

Two different samples were made by manual arc welding of the plates (dimensions 500 x 200 mm, one plate HSLA steel – NIOVAL 47 the other one – high alloyed austenite steel X7CrNiNb18.10, the filler metal INOX R 29/9, Jesenice steelworks) with the higher and lower heat input (samples 4 and 2, respectively). Specimens with two different crack positions, in HAZ and WM, were made and tested at two different temperatures, 20 °C and –60 °C. The electromechanical testing machine SCHENCK TREBEL RM 400 was used, including special inductive measurement unit for CTOD, with ± 0.01 mm accuracy.

Approximately 50 % of the final fatigue pre-cracking was done by maximal force  $F_{max} = 0.4 \cdot F_L$ , whereas the minimal force was  $F_{min} = 0.1 \cdot F_{max}$ . The high-frequency pulsator CRACKTRONIC was used, Fig. 10.



Figure 10. The high-frequency pulsator CRACKTRONIC

Results of fracture mechanics testings are shown in Figure 11 for a typical case, sample 2 (lower heat input), specimen with crack in WM, tested at 20 °C. When J-R curve is positioned in the same diagram as CDFs, obtained by King's method, Fig. 12, both the stress for stable crack initiation ( $\sigma_{init}$ ) and the initial crack length ( $a_{un}$ ) for unstable crack growth can be estimated. Crack Driving Forces, as shown in Figure 12, are expressed via J integral and given for different levels of loading, defined as a ratio of remote tensile stress and yield stress (0.2 – 1.0). Diagrams for other samples are given in [1].

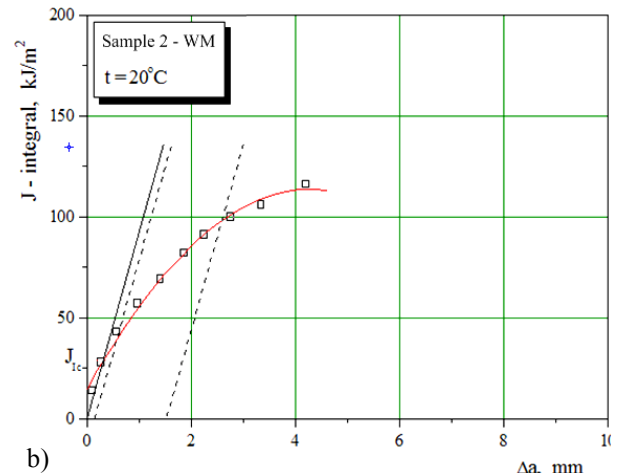
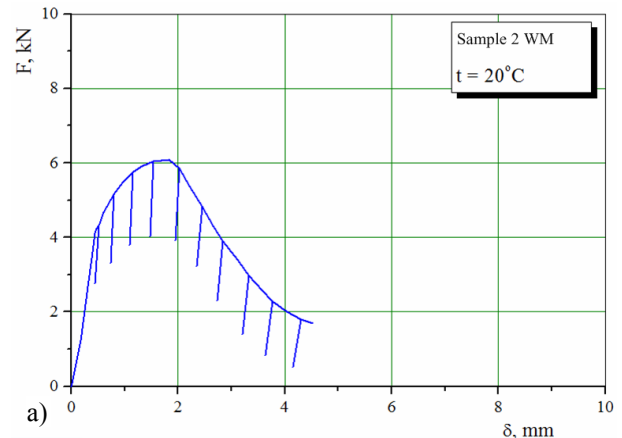
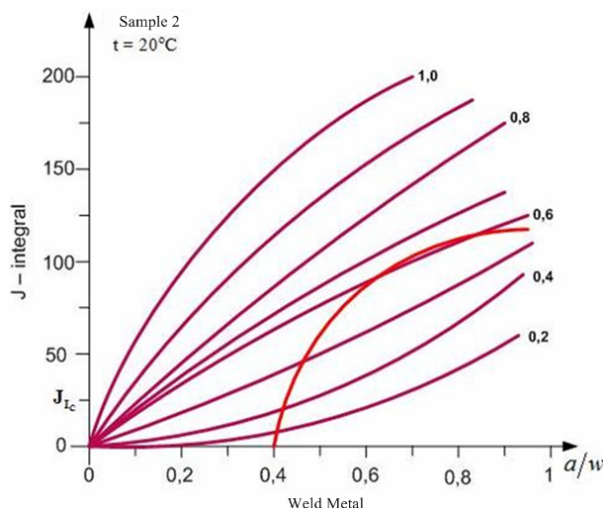


Figure 11. a) F-δ curve, b) J-R curve for sample 2, WM, 20 °C



**Figure 12. CDFs vs. J-R curve for sample 2, WM, 20 °C**

In the same way, all other samples were tested and the results shown in Table 1, where the stresses for the stable crack initiation ( $\sigma_{\text{inic}}$ ) and the crack lengths ( $a_{\text{un}}$ ) for the unstable crack growth are given for both samples, both crack tip positions (WM and HAZ) and both testing temperatures (20 °C and –60 °C).

**Table 1. Results of CDFs vs J-R curve analysis**

	WM 2	WM 4	HAZ 2 + 20 °C	HAZ 4 + 20 °C	HAZ 2 – 60 °C	HAZ 4 – 60 °C
$\sigma_{\text{inic}}$ [MPa]	264	319	298	306	264	285
$\sigma_{\text{inic}}/\sigma$	0.62	0.74	0.70	0.72	0.62	0.67
$a_{\text{un}}$ [mm]	7.2	7.5	8.2	7.7	6.8	6.4

## 6. CONCLUSIONS

Based on results presented here and in more details in [1], one can conclude the following:

- For the higher heat input  $\sigma_{\text{inic}}$  is always higher, while  $a_{\text{un}}$  is higher in WM, but smaller in HAZ, so the higher heat input is somewhat better;
- The HAZ of microalloyed steel has greater resistance against cracks than the WM, being quite different comparing e.g. to the behaviour of microalloyed steels welded joints;
- High stress levels for initiation of stable crack growth suggest the possibility that the welded structure can operate safely even in the presence of relatively large surface cracks;

- The integrity of heterogeneous welded joints is not affected by the presence of surface cracks because overmatching plays a protecting role, which consists of a small plastic deformation of weld metal even at high loads causing fracture of parent metal. The latest conclusion holds at low temperatures, as well.

## ACKNOWLEDGEMENTS

We acknowledge the support for this investigation by MESSER Tehnogas, AD, Beograd.

## REFERENCES

- [1] Jovicic, R.: *An analysis of the crack effect on the integrity ferrite-austenite welded joints*, PhD thesis, Faculty of Mechanical Engineering, University of Belgrade, Belgrade, 2007, (in Serbian).
- [2] Jovicic, R. et al.: *Report for the experimental investigation at Messer tehrogas*, Faculty of Mechanical Engineering, Belgrade, 2005, (in Serbian).
- [3] Sedmak, A.: *Application of fracture mechanics to structural integrity*, Faculty of Mechanical Engineering, Belgrade, 2003, (in Serbian).
- [4] ASTM E1820-99a Standard Test Method for Measurement of Fracture Toughness, Annual Book of ASTM Standards, Vol. 04.01, 1999.

## ПРОЦЕНА ИНТЕГРИТЕТА ФЕРИТНО-АУСТЕНИТИЧИХ ЗАВАРЕНИХ СПОЈЕВА

**Радомир Јовичић, Александар Седмак, Зајац Бурзић, Венцислав Грабулов, Јасмина Лозановић**

Овај рад приказује утицај преслине на интегритет хетерогених феритно-аустенитних заварених спојева применом основних принципа механике лома. Силе раста преслине су одређене нумерички применом Кингове методе, док је отпорност материјала на раст преслине одређена експериментално помоћу J-R криве. Да би се одредила својства оваквог завареног споја, заварене су плоче високолегираног аустенитног челика и микролегираног феритног челика. Експериментално истраживање, у комбинацији са нумерички добијеним резултатима, омогућило је процену интегритета феритно-аустенитних заварених спојева.